

## Characterization of LiF and CaF<sub>2</sub> surfaces using MIES and UPS (HeI)

D. Ochs<sup>a,\*</sup>, M. Brause<sup>a</sup>, S. Krischok<sup>a</sup>, P. Stracke<sup>a</sup>, W. Maus-Friedrichs<sup>a</sup>, V. Puchin<sup>b</sup>,  
A. Popov<sup>c</sup>, V. Kempter<sup>a</sup>

<sup>a</sup>Physikalisches Institut der TU Clausthal, Leibnizstraße 4, D-38678 Clausthal, Germany

<sup>b</sup>Institute of Chemical Physics, University of Latvia, Rainis Blvd. 19, Riga LV-1586, Latvia

<sup>c</sup>Institute of Solid State Physics, University of Latvia, Kengaraga Str.8, Riga LV-1063, Latvia

### Abstract

Metastable impact electron spectroscopy (MIES) and UPS (HeI) in combination with *ab initio* calculations (CRYSTAL-code) were applied to study surface and bulk defects in LiF and CaF<sub>2</sub>. The investigated stoichiometric, defective and doped surfaces are LiF, LiF doped with Mg, and CaF<sub>2</sub>. The experimental information obtained on the electronic structure of stoichiometric and defective surfaces of LiF (100), LiF on W (110) and CaF<sub>2</sub> (111) is discussed on the basis of the *ab initio* calculations. MIES spectra show features from Li agglomerates on the surface of electron bombarded LiF. The electronic structure of the LiF:Mg single crystal shows additional features above the valence band maximum caused by the Mg doping. These are identified as caused by the formation of (Mg–O) surface bonds. Exposure of CaF<sub>2</sub> surfaces to X-rays (1486 eV) shows also formation of metallic regions on the surface. © 1998 Elsevier Science B.V.

**Keywords:** Metastable impact electron spectroscopy (MIES); UPS; LiF; CaF<sub>2</sub>; ESD; PSD; *ab initio* electronic structure calculations

### 1. Introduction

During recent years the combination of the electron spectroscopy techniques metastable impact electron spectroscopy (MIES) ultra-violet photoelectron spectroscopy (UPS (HeI)) and UPS (HeI) was demonstrated to be useful in monitoring the changes in the electronic properties of surfaces during the growth of insulating films on metallic or semiconducting substrates [1–6]. Insulator surfaces are seldom defect free; the most common defects are point defects like anion vacancies in the case of ionic crystals and line defects like kinks, steps etc. MIES is capable of

giving information on the absolute position of surface defects with respect to the valence band (VB) maximum [7].

In this contribution the combination of MIES and UPS is applied to study the electronic properties of defects introduced systematically into insulating layers and bulk insulators (LiF, CaF<sub>2</sub>) by electron bombardment and by photons. LiF provides several outstanding point defects which are of great importance for technological application [8,9]. LiF with F-type colour centers is known as one of the important laser materials [9]. Thermoluminescence compounds on the basis of LiF:Mg (LiF:Mg [9], LiF:Mg,Tl [8–10] and LiF:Mg,Cu,P [11]) have been demonstrated to be excellent ionizing radiation dosimetry materials. Surface metallization of CaF<sub>2</sub> is of great interest for high resolution

\* Corresponding author. Email: Dirk.Ochs@tu-clausthal.de; Fax: +495323723600.

patterning of  $\text{CaF}_2$  crystals and films by photons [12] and electron beams [13–16]. The ultimate goal of such studies are structures of less than 2 nm size [17] for microstructures in the semiconductor industry.

Information on defects and dopants is obtained from a comparison of the electron spectra of defective and doped surfaces and the densities of states (DOS) at the surface and near-surface region. These DOS were calculated by *ab initio* techniques.

## 2. Experimental

For a description of the apparatus see Ref. [18] in this volume. Briefly, it is equipped with a cold-cathode gas discharge source for the production of metastable  $\text{He}^*(^3\text{S}/^1\text{S})$  ( $E^* = 19.8/20.6$  eV) atoms with thermal kinetic energies and HeI photons ( $E^* = 21.2$  eV) as a source for UPS.

The kinetic energies  $E_{\text{kin}} = 21.2$  eV (UPS) and  $E_{\text{kin}} = 19.8$  eV (MIES) displayed in the spectra correspond to electrons emitted from the Fermi level  $E_{\text{F}}$  of the substrate and correspond to a binding energy  $E_{\text{B}} = 0$  eV. Additionally the apparatus is equipped with the standard surface analytical tools X-ray photoelectron spectroscopy (XPS), Auger electron spectroscopy (AES) and low energy electron diffraction (LEED) XPS, AES and LEED.

MIES and UPS experiments on metal and insulator films grown on W(110) or Si(111) were performed biasing the target by 50 eV, which has been shown to have almost no influence on the spectral features. To avoid charge-up of the LiF(100),  $\text{CaF}_2(111)$  and LiF:Mg crystals a flood gun (hot tungsten filament) was operated behind the investigated crystals; a potential difference of 2 V was applied between the filament and the crystal. To clean the surface of the LiF(100) single crystal (MaTeck company) repeated heating–sputtering cycles were required in order to remove surface adsorbates. Thereby the crystal holder was heated to about 1000 K, and the  $\text{Ar}^+$  ions (500 eV;  $1 \mu\text{A cm}^{-2}$ ), incident under  $70^\circ$  with respect to the surface normal, were employed for sputtering. The cleanness of the crystal was checked with XPS as well as with MIES and UPS(HeI). The LiF films on W(110) were prepared as follows: LiF molecules are supplied to the clean W(110) substrate by

thermal evaporation (1100 K) of single crystal LiF chips. The thickness of the produced film is estimated as 10 nm on the basis of XPS measurements. At this thickness the electronic properties of the film, as judged from the MIES and UPS (HeI) measurements, resemble the bulk LiF(100) surface (see below).  $\text{CaF}_2(111)$  single crystals and LiF:Mg crystals were cleaved in air and then rapidly introduced to UHV.

Ca on Si(111) was prepared by evaporating Ca via a commercial Knudsen cell on the cleaned Si(111) surface. MgO on Si(100) surface was prepared as described in Ref. [5].

## 3. Theory

### 3.1. Methods for the interpretation of MIES and UPS spectra

The interpretation of the MIES results is based on the model introduced by Niehaus et al. in Ref. [19]. Briefly, only Auger Deexcitation (AD) of the  $\text{He}^*(1s2s)$  probe atom can take place when it approaches the insulator surface, most probably at a distance of 3 a.u.. A resonant electron transfer to the surface, being the precursor for the Auger capture process, is not possible due to the lack of states in resonance with the He2s orbital. A surface electron fills the He (1s) hole while the He (2s) electron is emitted carrying the excess energy. The transition probability is proportional to the density of occupied states involved in the AD process. The electron is emitted from the 2s state located at the He probe atom. Therefore, in contrast to UPS, the density of the empty states in the conduction band is of no concern for the interpretation of the MIES spectra. In a previous work on oxides we have already established that within the model of Niehaus et al. [19] the MIES spectra are well represented by the surface density of states (SDOS) of the valence band states [5,6]. Despite the fact that the UPS (HeI) spectra depend on the joint density of occupied and unoccupied states in the near-surface region, we compare the valence band DOS directly with UPS (HeI) spectra. This appears to be justified as long as we are mainly interested in global features, such as the general shape, the total width and position of the valence band spectrum.

### 3.2. Surface density of states

The density of states has been calculated using the CRYSTAL 95 computer code [20] designed for *ab initio* Hartree–Fock band structure calculations of periodic systems. However, up to now not much attention has been paid to the calculations of the surface density of states, which is relevant to the surface-sensitive systems like heterogeneous catalysts and electron spectroscopic methods such as MIES. The modifications of the densities of states (DOS) of LiF(100) surface induced by the atomic relaxation and by the presence of steps and kinks at the (100) surface have been investigated previously [21]. It was shown that the simulations correctly predict that the F2p peak in MIES spectra is narrower than in UPS spectra. This was shown to follow from the different depth of analysis: the MIES results are dominated by the emission of electrons from those states that protrude the most into the vacuum (i.e. the F2p<sub>z</sub> orbitals) while the UPS spectra are sensitive to the full F2p DOS in the near-surface region.

In this study we concentrate on MgF<sub>2</sub> and several composite superlattices derived from the LiF structure. In all cases Mg<sup>2+</sup> built into the LiF lattice is substituting one of the Li<sup>+</sup> ions in the expanded unit cell of LiF. The excess charge is compensated in different ways: (i) MgF<sub>2</sub>\*7(LiF) (Gavartin), Mg<sup>2+</sup> and the cation vacancy V<sub>c</sub> are in nearest lattice sites and form a hexagonal net within the (111) plane as suggested by Gavartin [22]; (ii) MgF<sub>2</sub>\*7(LiF) (interstitial), F<sup>-</sup> is inserted into a cubic interstitial site nearest to Mg<sup>2+</sup>; and (iii) MgO\*7(LiF): an O<sup>2-</sup> ion is replacing the F<sup>-</sup> located nearest to Mg<sup>2+</sup>.

The equilibrium structures, corresponding to the minimum of the total energy of the crystal, have been found using the least square fitting of the adiabatic potential surface by a quadratic form. The basis set for Li<sup>+</sup>, F<sup>-</sup>, Mg<sup>2+</sup> and O<sup>2-</sup> ions optimized for the bulk LiF, MgF<sub>2</sub> and MgO crystals is taken from Ref. [23]. In order to compare experimental electron spectra with the calculated density of states, broadening of the spectra due to different physical effects must be accounted for. We therefore used a Gaussian-shaped phonon broadening of FWHM = 1 eV, which has already been applied for oxide insulators [5,6].

Some *ab initio* calculations for CaF<sub>2</sub> with and

without F centers are known to us [24,25]; more detailed calculations are in progress [26].

## 4. Results and discussion

### 4.1. Electron bombarded LiF

Fig. 1 shows the MIES spectra of LiF/W(110): as prepared (1); after electron bombardment (2); and after additional heating the sample to about 600 K for 5 min (3). Fig. 2 (1) shows MIES results for LiF (100).

The MIES spectrum of the LiF(100) displays valence band emission with a pronounced maximum around a binding energy  $E_B = 9.5$  eV from ionization of F2p orbitals. The top of the valence band is found about 8.0 eV below  $E_F$ . The MIES spectrum of LiF on W(110) is very similar to that of LiF(100). Because

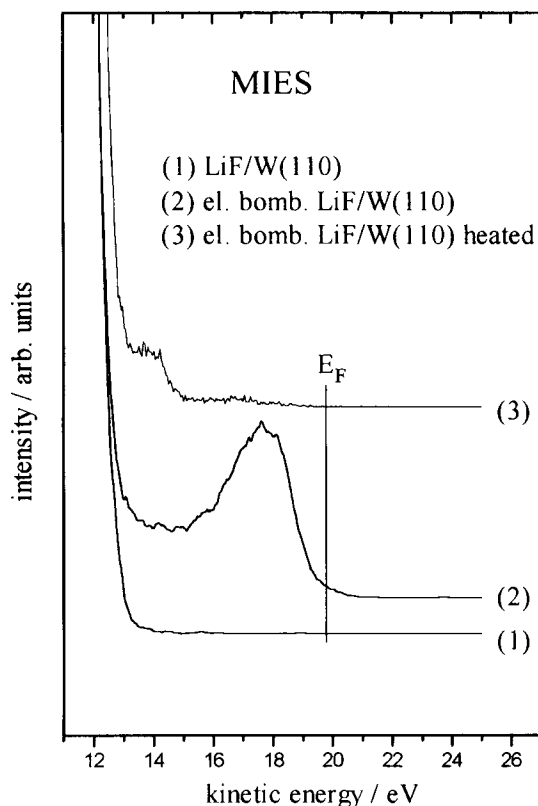


Fig. 1. MIES spectra of LiF/W (110): as prepared (1); after electron bombardment (2); after additional heating to about 600 K (3).

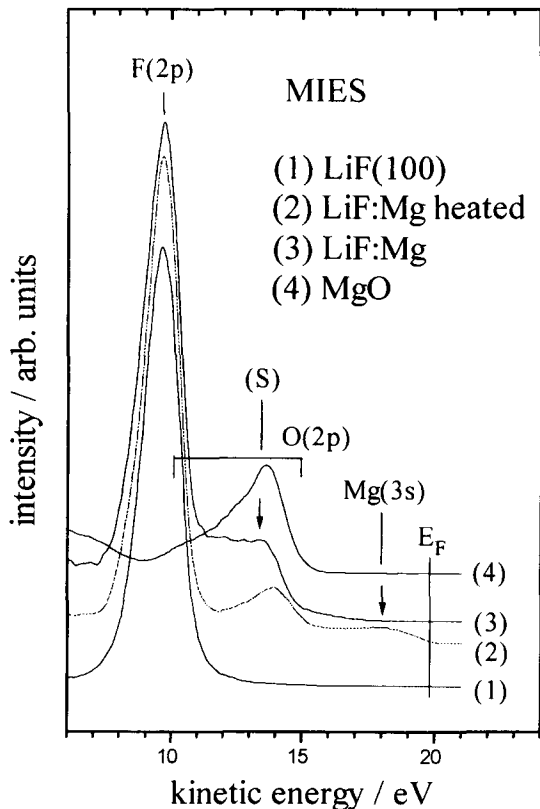


Fig. 2. MIES spectra of LiF (100) (1), LiF doped with Mg (LiF:Mg) before (3) and after (2) heating. For comparison a MgO spectrum is shown (4).

we are mainly interested in the identification of the smaller features in the spectra of Fig. 1, we only show the spectra starting from 12 eV kinetic energy.

The MIES data (Fig. 1 (2)) obtained after the dosing of an approx. 3 nm thick LiF film on W(110) with electrons (500 eV;  $10^{16}$  electrons  $\text{cm}^{-2}$ ) show an additional structure directly below the Fermi level centered about 5 eV above the top of the valence band. This structure is caused by ionization of the Li(2s) orbital. UPS (HeI) spectra (not shown here), taken simultaneously with the MIES spectra, show the VB emission only; Li(2s) is not seen in the UPS spectra.

We give the following interpretation: The peak emerging during the electron dosing of the LiF film is caused by electron transfer to the metastable probe atom connected with the formation of  $\text{He}^{-*}$  ( $^2\text{S}$ ) followed by autodetachment of the temporary ion.

For such doses a partial metallization appears to be well established [27,28]. We find however that the valence band (F(2p)) emission is attenuated by not more than 20%. This shows that no uniform adlayer has developed. Instead, metallic clusters or colloids are formed (see Ref. [27,28]).

After heating the bombarded sample (Fig. 1 (3)) to about 600 K the Li (2s) peak disappears. Some emission remains however visible above the top of the valence band when Li (2s) has disappeared. A peak at  $E_B = 5.5$  eV is found. We attribute this feature to the oxygenation of the metallic regions by background molecules, in particular  $\text{CO}_2$  and CO. This interpretation is based on: (i) our observation of a very similar structure during the oxygenation of Li adlayers on tungsten [29]; and (ii) Jardin et al. [30], who have concluded that Li atoms present on the top of a damaged LiF surface are oxidized in the ambient vacuum. Increasing the temperature above about 1000 K, the LiF film is removed completely.

#### 4.2. Mg doped LiF

Fig. 2 shows MIES spectra of Mg doped LiF (estimated Mg concentration of about  $10^{19} \text{ cm}^{-3}$ ) as prepared (3) and after heating to about 1000 K for several minutes (2), and MgO films on Si(100) (4). For the Mg doped LiF crystal the structure, labeled F(2p), is present as for the stoichiometric LiF(100) surface (see Fig. 2 (1)). Therefore we conclude that it is also due to F2p ionization.

In contrast to LiF(100) we find an additional shoulder (denoted as structure (S)) above the F2p valence band. This additional emission is confined to energies below about 3 eV above the top of the valence band emission. An interpretation of (S) will be offered on the basis of a comparison with the results of Fig. 3, which shows the total DOS for the defect structures described in Section 3.2 together with that of pure LiF and  $\text{MgF}_2$  crystals. The DOS in the F(2p) valence band is virtually the same in all cases. The additional states within the LiF band gap are due to the 2p states of the interstitial  $\text{F}^-$  ion in the case of  $\text{MgF}_2 \cdot 7(\text{LiF})$  interstitial structure and due to the O (2p) states in the case of  $\text{MgO} \cdot 7(\text{LiF})$ . The important finding is that  $(\text{Mg}_c^{2+} - \text{V}_a)$  (anion vacancy) dipoles produce no DOS in the bandgap of LiF(100);

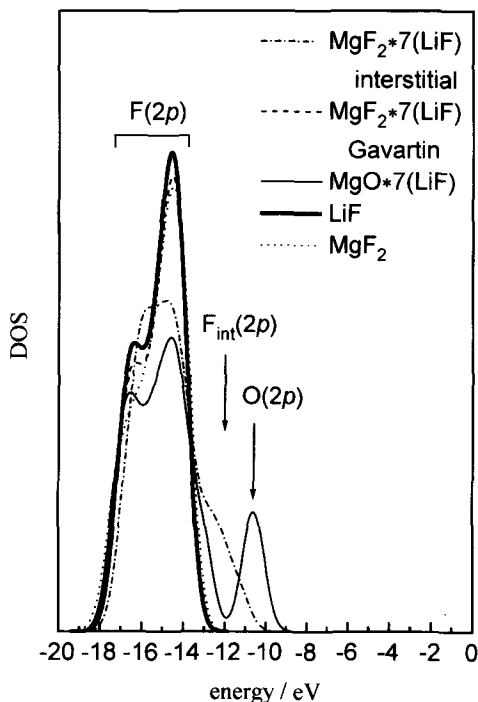


Fig. 3. Calculated density of states (valence band region only) in LiF,  $\text{MgF}_2$  and LiF:Mg.

the defect structures merely produce small modifications within the valence band.

The comparison of Fig. 2 with the numerical results of Fig. 3 shows a rather satisfactory agreement as far as the shape and width of the F2p valence band structure is concerned (for details see Ref. [21]).

Our numerical results appear to exclude  $(\text{Mg}^{2+}-V_c)$  impurity–vacancy dipoles as the origin for structure (S). They suggest that these defects produce merely resonances embedded into the valence band states, which are unlikely to be visible with the applied techniques.

The simulations furthermore show that Mg impurity– $\text{F}^-$  dipoles (interstitial structure) [31] indeed produce states located in the band gap of regular LiF (about 2.5 eV above the valence band maximum (see arrow)). Therefore, in principle, such defects could contribute to structure (S). However, we discard these defects as the main source for (S) with the following arguments: (i) the formation energy for the interstitial phase is much larger than that for the vacancy-rich structures; (ii) the volume increase due to the large concentration of the interstitial ions have

not been observed experimentally; and (iii) there is apparently no reason why the interstitial defects should be confined to the surface. Thus, structure (S) should be more prominent in the UPS than in the MIES spectra because UPS probes the sample several monolayers below the surface while MIES is exclusively surface-sensitive. UPS measurements (not shown here) do not show a more prominent structure (S).

We arrive at a possible explanation for structure (S) by taking into account: (i) our MIES/UPS results for MgO surfaces [5]; and (ii) the calculation of the energetic position of  $(\text{Mg}_c-\text{O}_a)$  centers in MgO doped LiF crystals (Ref. [1] and results for defect structure (iii)). In the following we will demonstrate that the results for LiF:Mg can be explained consistently by assuming that Mg species present at the surface of LiF:Mg react with oxygen containing molecules of the ambient vacuum, thus producing in this way  $(\text{Mg}-\text{O})$  bonds at the surface.

In order to analyze the adsorption and luminescence spectra of LiF–MgO crystals, the energetic position of  $(\text{Mg}_c-\text{O}_a)$  centers was calculated [32]. The calculation predicts that these centers induce occupied states around 2.7 eV above the valence band maximum of stoichiometric LiF. Thus, the position of the  $(\text{Mg}_c-\text{O}_a)$  centers agrees closely with the position of structure (S) for LiF:Mg. Moreover, it is found quite generally that oxygen defects in fluoride crystals generate states localized above the top of the valence band maximum [33]. Summarizing, the available evidence from experiment and calculation suggests that the Mg induced defects at the surface of LiF:Mg are  $(\text{Mg}-\text{O})$  centers.

Heating the surface to about 1000 K (Fig. 2 (2)) an additional structure (labeled Mg(3s)) appears in the MIES spectrum at and directly below the Fermi level  $E_F$ . Similar emission at the Fermi level was observed after bombarding LiF films with electrons (see above). Apparently, the intensity at the Fermi level signals again the presence of metallic regions on the surface. Such metallic regions are not produced, even for temperatures of 1000 K, on a regular LiF surface. Therefore, we suppose that these regions consist of Mg species which have diffused to the surface at elevated temperatures. A second feature of the heated LiF:Mg crystal is a peak at  $E_B = 6$  eV. The electronic structure of MgO (4) shows a peak at

the same position, therefore we assign the peak to metallic areas on the surface which are oxidized by the residual gas (CO, CO<sub>2</sub>). The results obtained for MgO\*7(LiF) (see Fig. 3) strongly support this picture.

#### 4.3. Photon irradiated ( $h\nu = 1486$ eV) CaF<sub>2</sub>

Fig. 4 displays the MIES spectra of CaF<sub>2</sub> (111) after photon irradiation ( $h\nu = 1486$  eV) (2) and after additional heating of the sample to about 600 K (1), Ca layers (thickness > 20 nm) on Si (111) (3), and Ca/Si(111) after exposure to about 300 L O<sub>2</sub> (4). Fig. 5 shows the corresponding UPS spectra. The MIES spectrum of irradiated CaF<sub>2</sub> shows a structure at and below the Fermi energy  $E_F$ , similar to that of the Ca on the Si (111) spectrum (1). The small contribution in

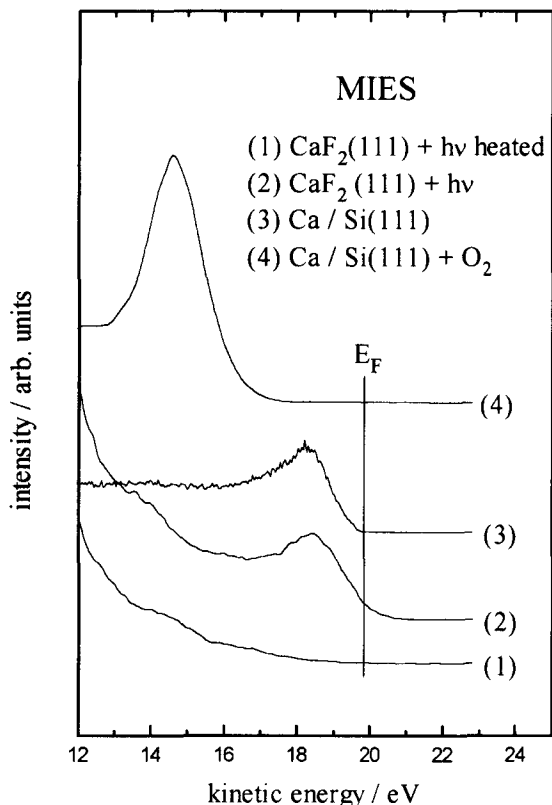


Fig. 4. MIES spectra of irradiated CaF<sub>2</sub> (111) before (2) and after (1) heating to about 600 K, Ca on Si (111) (Ca layer thickness > 20 nm) (3) and Ca/Si (111) exposed to about 300 L O<sub>2</sub> (4).

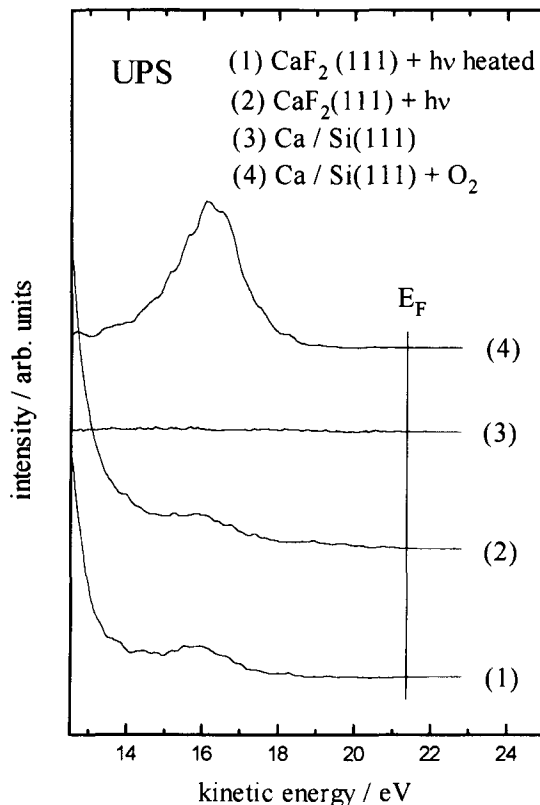


Fig. 5. UPS spectra of irradiated CaF<sub>2</sub> (111) before (2) and after (1) heating to about 600 K, Ca on Si(111) (Ca layer thickness > 20 nm) (3) and Ca/Si (111) exposed to about 300 L O<sub>2</sub> (4).

(2) just beyond  $E_F$  is due to the Auger de-excitation involving He ( $2^1S$ ) atoms (contributing about 14% to the total beam intensity). Because the emission in (2) extends to  $E_F$ , this indicates that the surface develops metallic properties during irradiation. Purely metallic patches, at least large enough to form a metallic band structure, develop.

A peak at  $E_B = 5.2$  eV is seen in the MIES and UPS spectra of (1) and (2). MIES and UPS spectra (4) for oxidized Ca on Si (111) show the same structure caused by O2p ionization. We attribute the structure at  $E_B = 5.2$  eV to the formation of (Ca–O) complexes (see also Ref. [24]): as soon as metallic areas are formed on the irradiated CaF<sub>2</sub> sample, the surface becomes very reactive against oxidation by adsorbates present on the *ex-situ* cleaved sample and the residual gas in the UHV. It could be shown that CaF<sub>2</sub> samples cleaved in UHV show smaller oxygen features [34].

In summary, photon-irradiated  $\text{CaF}_2$  surfaces show two new features similar to those found for electron bombarded LiF (see Section 4.1). These are attributed to the formation of metallic areas on the surface and their reaction with oxygen atoms.

## 5. Summary

The electronic structure of the surface of defective LiF (after electron bombardment and doped with Mg) and defective  $\text{CaF}_2$  (111) (after photon irradiation) was studied with the electron spectroscopic techniques MIES and UPS (HeI). For the LiF-based surfaces an interpretation of the results was made on the basis of *ab initio* calculations (also presented in this work) which model the studied surfaces. In all studied cases the spectra are dominated by the  $\text{F}2p$  valence band emission. On electron bombarded LiF and photon irradiated  $\text{CaF}_2$  we detect, in addition, emission close to the Fermi level which we attribute to the presence of Li patches on the surface. Another feature about 6 eV below  $E_F$  could be identified by comparison with our measurements on MgO and CaO as oxygen species at the surface presumably originating from molecules of the residual gas. Mg doped LiF shows only the feature 6 eV below  $E_F$  which we attribute to (Mg–O) surface complexes; after heating the surface to about 1000 K a structure near the Fermi energy develops which could be identified as Mg patches on the surface.

## Acknowledgements

Financial support of the Deutsche Forschungsgemeinschaft is gratefully acknowledged (Ke 155/24 and 436 LET 113/1). The calculations have been performed at the Regionales Rechenzentrum für Niedersachsen (RRZN) in Hannover.

## References

- [1] H. Ishii, S. Masuda, Y. Harada, Surf. Sci. 239 (1990) 220.
- [2] A. Hitzke, S. Pülm, H. Müller, R. Hausmann, J. Günster, S. Dieckhoff, W. Maus-Friedrichs, V. Kempter, Surf. Sci. 291 (1993) 67.
- [3] S. Pülm, A. Hitzke, J. Günster, W. Maus-Friedrichs, V. Kempter, Surf. Sci. 325 (1995) 75.
- [4] S. Pülm, A. Hitzke, J. Günster, H. Müller, V. Kempter, Rad. Eff. Def. Sol. 128 (1994) 151.
- [5] D. Ochs, W. Maus-Friedrichs, M. Brause, J. Günster, V. Kempter, V. Puchin, A. Shluger, L. Kantorovich, Surf. Sci. 365 (1996) 557.
- [6] V.E. Puchin, J.D. Gale, A.L. Shluger, E.A. Kotomin, J. Günster, M. Brause, V. Kempter, Surf. Sci. 370 (1996) 190.
- [7] V. Kempter, Materials Science Forum, vols. 239–241, Defects in Insulating Materials (ICDIM 1996), p. 621. ISSN 0255-5476 (Trans Tech Publications, 1997).
- [8] F. Agullo-Lopez, C.R.A. Catlow, P.D. Townsend, Point Defects in Materials, Academic Press, 1988.
- [9] S.W.S. McKeever, Thermoluminescence of Solids, Cambridge University Press, Cambridge, 1985.
- [10] T.G. Stoebe, S. Watanabe, Phys. Stat. Sol. (a) 29 (1975) 11.
- [11] G. Chen, F. Wu, Y. Li, J. Zha, Radiat. Prot. Dosim 14 (1986) 223.
- [12] M. Oshima, S. Maeyma, H. Takenada, Y. Ishii, H. Sugahara, J. Vac. Sci. Tech. A10 (1992) 163.
- [13] T.R. Harrison, P.M. Mankiewich, A.H. Dayem, Appl. Phys. Lett. 41 (1982) 1102.
- [14] P.M. Mankiewich, H.G. Craighead, T. R Harrison, A.H. Dayem, Appl. Phys. Lett. 44 (1984) 468.
- [15] M.A. McCord, R.F.W. Pease, J. Vac. Sci. Tech. B5 (1987) 430.
- [16] Y. Hirose, S. Horng, A. Kahn, C. Wrenn, R. Pfeffer, J. Vac. Sci. Tech A10 (1992) 960.
- [17] M. Isaacson, A. Murray, J. Vac. Sci. Tech. 19 (1981) 1117.
- [18] D. Ochs, M. Brause, W. Maus-Friedrichs, V. Kempter, ICES-7, J. El. Spec. Rel. Phen. same volume!
- [19] P.A. Zeijlmans van Emmichoven, P.A.A.F. Wouters, A. Niehaus, Surf. Sci. 195 (1988) 115; P. Eeken, J.M. Fluit, A. Niehaus, I. Urazgildin, Surf. Sci. 273 (1992) 160; H. Brenten, H. Müller, A. Niehaus, V. Kempter, Surf. Sci. 278 (1992) 183.
- [20] R. Dovesi, C. Pisani, C. Roetti, M. Causá, V.R. Saunders, CRYSTAL-88, QCPE program No. 577, Bloomington IN, 1989; C. Pisani, R. Dovesi, C. Roetti, Hartree–Fock Ab-initio Treatment of Crystalline Systems, Lecture Notes in Chemistry, Springer, Heidelberg, 1988.
- [21] D. Ochs, M. Brause, P. Stracke, S. Krischok, F. Wieggershaus, W. Maus-Friedrichs, V. Kempter, V. Puchin, A. Shluger, Surf. Sci. 383 (1997) 162.
- [22] J.L. Gavartin, E.K. Shidlovskaya, A.L. Shluger, A.N. Varaksin, J. Phys.: Condens. Matter 3 (1991) 2237.
- [23] M. Causa, R. Dovesi, F. Ricca, Surf. Sci. 280 (1993) 1; A. Pavese, R. Dovesi, C. Roetti, M. Causa, Phys. Rev. B44 (1991) 3509; M. Causa, R. Dovesi, C. Pisani, C. Roetti, Phys. Rev. B33 (1986) 1308.
- [24] A.V. Puchina, V.E. Puchin, E.A. Kotomin, M. Reichling, Int. Cent. Theor. Phys., Trieste IC/97/112 and ECOSS-17, WeP49.
- [25] E. Westin, A. Rosen, E. Matthias, Springer Ser. Surf. Sci. Vol. 19 (1990) 316.
- [26] V. Puchin, in preparation, not published yet.

- [27] Dou Onn, D.W. Lynch, A.J. Bevolo, *Surf. Sci.* 219 (1989) L623.
- [28] N. Seifert, Ye Hui, D. Lin, R.G. Albridge, A.V. Barnes, N. Tolk, W. Husinsky, G. Betz, *Nucl. Instr. Meth. B* 72 (1992) 401.
- [29] W. Maus-Friedrichs, S. Dieckhoff, M. Wehrhahn, S. Pülm, V. Kempter, *Surf. Sci.* 271 (1992) 113.
- [30] C. Jardin, P. Durupt, J. Davenas, *Radiat. Eff. Def. Sol.* 137 (1995) 29.
- [31] S.S. de Souza, A.R. Blak, *Materials Science Forum*, vols. 239–241, ISSN 0255-5476 (Trans Tech Publications, 1997) Defects in Insulating Materials (ICDIM 1996), p. 699.
- [32] S.N. Mysovskii, S.N. Mironenko, I. Nepomnyashchikh, A.L. Shluyger, *Opt. Spectroscop. (USSR)* 63 (1987) 478.
- [33] E. Radzhabov, *Materials Science Forum*, vols. 239–241, Defects in Insulating Materials (ICDIM 1996), p. 261. ISSN 0255-5476 (Trans Tech Publications, 1997).
- [34] M.Reichling, M. Huisinga, D. Ochs, V. Kempter, ECOSS-17, Enschede (1997) accepted for publication in *Surf. Sci.*, 1998.